EUROPEAN MECHANICAL SCIENCE
e-ISSN: 2587-1110

RESEARCH ARTICLE

Evaluating the effectiveness of combined hardening models to determine the behavior of a plate with a hole under combined loadings

Melih Çaylak[1], Toros Arda Akşen[1], Mehmet Firat[1*]

[1]The University of Sakarya, Department of Mechanical Engineering, Sakarya, Turkey

Orcid: M. Çaylak (0000-0002-6857-6642), T.A. Akşen (0000-0002-7087-3216), M. Firat (0000-0002-3973-4736)

Abstract: Geometrical discontinuities in a material such as holes and notches on machine elements are called as critical regions due to the stress concentrations. They are the potential failure initiation locations, therefore, researchers put significant effort on the prediction of the material response in these discontinuities, especially under repetitive loadings. Cyclic plasticity is an important field of computational mechanics and deals with the nonlinear material response under cyclic loadings. In this study, numerical cyclic stress – strain response of a plate with a hole was evaluated under the combined loadings which are cyclic bending and tensile loadings. Oxygen Free High Thermal Conductivity (OFHC) Copper alloy was considered as material, and finite element simulations were performed in Marc software. A user defined material subroutine known as Hypela2 was utilized in order to define the material response. The plasticity model used in the present study comprises J2 plasticity along with combined isotropic – kinematic hardening model. Evolution of the backstress was introduced by Armstrong – Frederic type kinematic hardening model. The results were compared with the literature study, and it was seen that presented hardening model provides accurate results in small cyclic strain range.

Keywords: Cyclic Plasticity, Armstrong-Frederic Model, Kinematic Hardening, Small Strain, Finite Element Method

1. Introduction

Cyclic plasticity is an important research field investigating the stress – strain behavior of the materials under repetitive loadings. Under cyclic loading, materials exhibit unique features such as Bauschinger effect and ratcheting response. In order to model both behaviors, kinematic hardening models are incorporated into the constitutive framework. Prager [1] introduced the first kinematic hardening model. This linear kinematic hardening model could predict the Bauschinger effect; however, it fails to model the ratcheting. Later, Besseling [2] and Mroz [3] proposed multi-surface kinematic models based on the modifications of the Prager's model. However, both models could not tackle the ratcheting behavior. There were also several models based on multi-surface concept have been proposed in the literature [4, 5]. Then, Armstrong – Frederic put forward a nonlinear kinematic hardening model to sort out the ratcheting issue taking a fading memory – recovery term into consideration [6]. Through the fading memory term, backstress could saturate at a constant value and this model could present the ratcheting behavior of the material.

Some works can be found in the literature evaluating the influence of the kinematic hardening models on the cyclic stress – strain response of the material. Firat [8] carried out the finite element (FE) simulations of a notched round bar to investigate the notch root strains under combined loadings. 20 different tests comprising of proportional and non-proportional loadings were considered for SAE1070 steel. A kinematic hardening model in conjunction with a yield surface in pseudo stress space was implemented. It was observed that the numerical results were consistent with the experimental outcomes. Firat [9] also carried out another study on the same notched round bar using von Mises yield criterion coupled with a kinematic hardening model with multi – component. Six proportional and non-proportional tests were simulated in this study, he reported that the numerical results were consistent with the experiments and the presented material model was suitable for the fatigue life estimation. Aksen et. al. [10] conducted similar study on the same circumferentially notched round bar and assessed the effect of the different backstress parameters on the cyclic response of the material subjected to combined proportional and – non-proportional loadings. Joo and Huh [11], evaluated the stress – strain behavior of TWIP980

* Corresponding author.
Email: firat@sakarya.edu.tr

European Mechanical Science (2022), 6(2): 97-104
https://doi.org/10.26701/ems.1051057
Received: December 13, 2021 — Accepted: February 8, 2022

and TRIP980 steel sheets numerically and experimentally, under monotonic tensile and reversal tensile – compressive loadings. They employed a rate dependent material model involving a combined isotropic and kinematic hardening model in numerical approach to characterize the Bauschinger effect along with the transient behavior of the material. It was recorded that the proposed material model can be adopted in sheet metal forming applications as well as springback prediction. Huh et. al. [12] investigated the cyclic behavior of DQ and DP590 steels under intermediate and different strain rates by using combined hardening model. In addition, both FE simulations and experiments were conducted for different complex loading paths. The dependency of Bauschinger effect on strain rate was also evaluated and it is concluded that the Bauschinger effect changes with strain rates. Ohno et al. [13] developed a new algorithm to minimize ratcheting and cyclic stress relaxation. To this end, a plate with a hole was considered and finite element analyses were conducted for different element types such as brick and shell element to prove the accuracy of the new algorithm. An annealed OFHC Copper was chosen as material in this study and a combined hardening model was adopted as a hardening rule. It was reported that the new algorithm is applicable to both two-dimensional and three-dimensional stress states. Zhang et. al. [14] conducted a study by using the same specimen to introduce a new hardening model for cyclic plasticity, which takes into account anisotropic nonlinear kinematic and nonlinear isotropic hardening. It was concluded that, with the new model, predictions are mostly suitable even for the different materials and different loading paths. Montáns and Zhang [15] also carried out another study on the same holed plate made of OFHC Copper. They proposed a new model for non-linear kinematic hardening at large strains. It was reported that the new approach is suitable for large strains for soft materials and has no restriction tackling the materials anisotropy or the form of the stored energy. Fu et. al. [16] investigated the ratcheting effect of thin steel wires under cyclic loading comprising of tension-torsion loading. Experiments were conducted for thin 316L steel wires under different loading conditions. Finite element (FE) simulations with different kinematic hardening rules were also conducted. It was pointed out for macro-based model's that the numerical results tend to under-estimate the ratcheting behavior. Shojaei et. al. [17] applied a combined hardening model to predict ratcheting behavior of CS1026 steel under cyclic loading. Experimental data and numerical solutions were compared in this study. It was reported that the hardening rule used in the work accomplished to describe the material behavior under different repetitive loading paths. Badvana et. al. [18] investigated the ratcheting response of SS304 stainless steel numerically and experimentally under cyclic loading. To predict plastic behavior of the material, a combined hardening model and von-Mises isotropic yield criterion were employed. It was reported that, proposed hardening model satisfactorily predicted the experimental results. Tasavori et. al. [19] conducted similar study on 9Cr-1Mo steel in order to evaluate the ratcheting behavior under cyclic loadings. Numerical results predicted from the presented combined hardening model were compared with and the experimental outcomes. It was reported that accumulate progressive plastic strain is observed and amount of accumulated plastic strain is related with geometry of specimens. Nath et. al. [20] investigated the ratcheting effect on cyclically stable materials under different loading conditions. The results predicted by employing the introduced combined hardening model and the experimental outcomes were compared in this work. As a result, it was reported that the hardening data obtained with the presented method showed a good agreement with the experimental data. Lee et. al. [21] investigated the directional dependency of the hardening response. Several FE analyses were carried out for different material orientations. A new combined hardening model accounting for the directional dependency of the Bauschinger effect was proposed and compared with the existing literature It was reported that new model provides superior performance. Qin et. al. [22] proposed a new combined hardening model to examine the behavior of aluminums and steels under complex strain paths. They compared the numerical results with the experimental data for EDDQ pure aluminum and DP780 steel. It was pointed out that the accuracy of the proposed model for representing the Bauschinger effect, transient hardening and permanent softening under different strain paths is sufficient for the related materials. There are also several works investigating the effect of the combined hardening for different applications of mechanical design [23-25] and investigating the cyclic behaviors of notched specimens [26].

In this work, finite element (FE) analyses of a centered hole plate were conducted using a material model comprising an isotropic yield criterion in conjunction with Armstrong – Frederic kinematic hardening model. Oxygen Free High Thermal Conductivity (OFHC) Copper was considered as a test material. The plate was subjected to the tensile loading and bending, simultaneously. The results were compared with the numerical outcomes of Ohno.

2. Constitutive Model

A plasticity model involves a yield criterion, a flow rule, and a hardening rule. Yield criterion represents a limit distinguishing the elastic and plastic domains from each other. Flow rule establishes a relationship between the stress increment and plastic strain increment. Lastly, hardening rule elucidates the change of yield surface in terms of motion and expansion. In the present study, von Mises yield criterion was employed as yield function, and this criterion can be expressed as follows.

$$f_{VM} = \sqrt{\frac{2}{3}(\underline{\underline{S}} - \underline{\underline{\alpha}}) : (\underline{\underline{S}} - \underline{\underline{\alpha}})} - \sigma_0 = 0 \quad (1)$$

where, S denotes the deviatoric component of the stress tensor and α is the backstress tensor. σ_0 is the yield stress which is a function of the equivalent plastic strain. Here, the deviatoric component of stress can be defined as Eq. (2).

$$\underline{\underline{S}} = \underline{\underline{\sigma}} - \underline{\underline{\lambda}}\sigma_m \quad (2)$$

Here, λ is the Kronecker delta and σ_m is the mean stress. σ refers to the Cauchy stress tensor. Strain can be disintegrated into elastic and plastic components in an additive way such that,

$$d\underline{\underline{\varepsilon}} = d\underline{\underline{\varepsilon}}_e + d\underline{\underline{\varepsilon}}_p \quad (3)$$

Cauchy stress tensor can be determined using Hooke's law as follows.

$$d\underline{\underline{\sigma}} = \underline{\underline{\underline{\underline{C}}}}_e : d\underline{\underline{\varepsilon}}_e \quad (4)$$

Here C_e is the elastic tensor. Associated flow rule used in this work and is given in Eq. (5).

$$d\underline{\underline{\varepsilon}}_p = d\lambda \frac{df}{d\underline{\underline{\sigma}}} \quad (5)$$

In the equation above, $d\lambda$ denotes the plastic proportionality factor. During the plastic deformation, the yield locus expands, and the Cauchy stresses should comply with the expansion of the yield locus which leads to,

$$df = \frac{df}{d\underline{\underline{\sigma}}} : d\underline{\underline{\sigma}} + \frac{df}{d\bar{\varepsilon}_p} : d\bar{\varepsilon}_p = 0 \quad (6)$$

Hardening rule is essentially employed in order to capture the Bauschinger effect, ratcheting response. Initial attempts are concentrated on the modeling of Bauschinger effect [1, 7]. Later, Armstrong and Frederic proposed another model (AF) in order to predict the ratcheting behavior [6]. AF Kinematic hardening model can be expressed by Eq. (7).

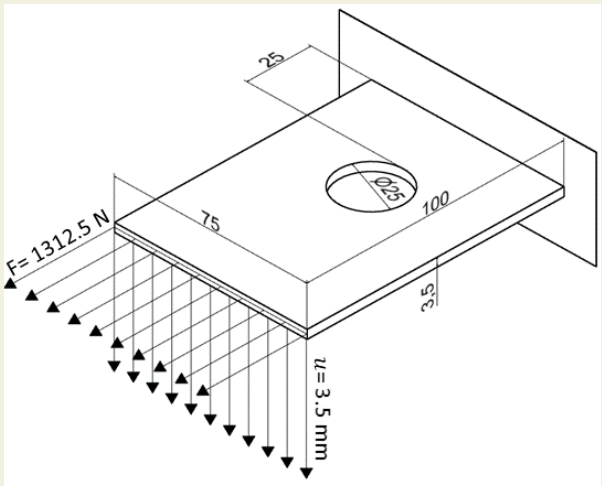

Figure 1. Model description [13]

$$d\underline{\underline{\alpha}} = \frac{2}{3} C d\underline{\underline{\varepsilon}}_p - \gamma\alpha\sqrt{\frac{2}{3} d\underline{\underline{\varepsilon}}_p : d\underline{\underline{\varepsilon}}_p} \quad (7)$$

The equation above comprises of two components. The first one represents the linear hardening; the second term represents the dynamic recovery [27]. Owing to the dynamic recovery term, AF model could represent the ratcheting behavior of the material. Hardening modulus decreases gradually and backstress eventually saturates at a constant value of C/γ. Here C and γ are correlated with the kinematic hardening part of the combined hardening model.

AF model was incorporated into the FE simulations through Hypela2 user defined material behavior subroutine.

3. Application

3.1. Description of the Model

In the present work, FE simulations of a plate with a hole were carried out. Dimensions of the model were procured from the Ref [13]. A tensile force of 1312.5 N was applied to the specimen which leads to 5 MPa nominal stress on one edge of the plate, while the other edge was fixed in all directions. Simultaneously, the same edge exposing to the constant nominal stress was subjected to the cyclic bending as well. The cyclic bending was applied as a displacement in out of plane direction. Fig. 1. shows the dimensions and loading conditions of the plate

Loading conditions were presented in Fig. 2 for tensile and bending loadings, separately.

3.2. Characterization of the Material

Within the scope of this work, OFHC copper was used as a test material. The mechanical data of the OFHC copper was taken from the Ref [13] and listed in the Table 1. Materials hardening curve was characterized by Swift law which is expressed as in the Eq. (8).

Table 1. Mechanical properties of OFHC Copper [13]

Parameter	Value
Swift Coefficient of Strength (K)[MPa]	144
Swift Hardening Exponent (n)	0.2
Reference strain (ε_0)	0.000011
Young Modulus [MPa]	123000
Poisson Ratio	0.34

$$\sigma_{true} = K.\left(\varepsilon_0^p + \varepsilon^p\right)^n \quad (8)$$

Combined hardening was adopted to represent the behavior of the material under cyclic loadings. Parameters of the combined hardening law were obtained using curve fitting method as well. Hardening was assumed as sum of the initial yield stress, backstress and isotropic hardening curve. The parameters of combined hardening law were

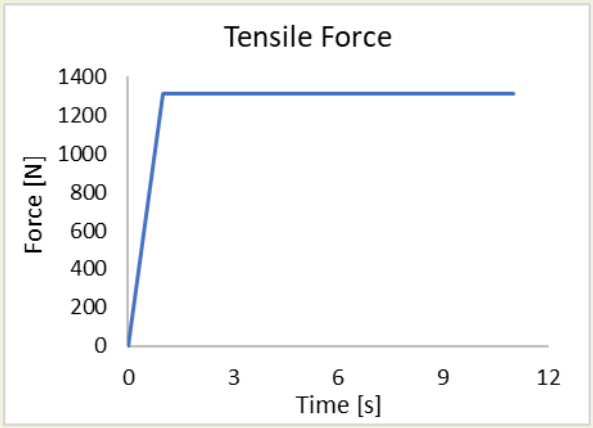

a)

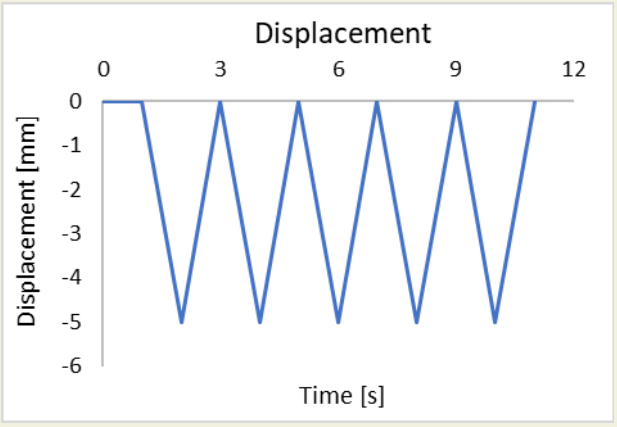

b)

Figure 2. Loading conditions for a) Tension b) Bending

summarized in Table 2. Isotropic hardening and backstress curves generated using these parameters were illustrated in Fig. 3. The expression of combined isotropic – kinematic hardening is as follows:

$$\sigma_{true} = \sigma_0 + \frac{Q}{b}\left(1 - e^{-b\varepsilon_p}\right) + \frac{C}{\gamma}\left(1 - e^{-\gamma\varepsilon_p}\right) \quad (9)$$

σ_0 denotes the initial yield stress whereas C and γ are the kinematic hardening parameters of AF model. Q and b are associated with the isotropic hardening behavior of the material.

Table 2. Combined hardening parameters of OFHC Copper

Parameters	σ_0 [MPa]	Q[MPa]	b	C [MPa]	γ
Value	14.67	2060	40	26000	1000

3.3. Ohno Model

In the present study, Ohno's model was utilized only for the comparison. Only a brief explanation was given here. Ohno disintegrated the backstress into several components. The backstress introduced by Ohno is as follows.

$$d\underline{\underline{\alpha}}^{(i)} = \frac{2}{3}h^{(i)}d\underline{\underline{\varepsilon}}^{p} - \zeta^{(i)}\left(\frac{\underline{\underline{\alpha}}^{(i)}}{r^{(i)}}\right)^{k^{(i)}}\alpha^{(i)}dp \quad (10)$$

where,

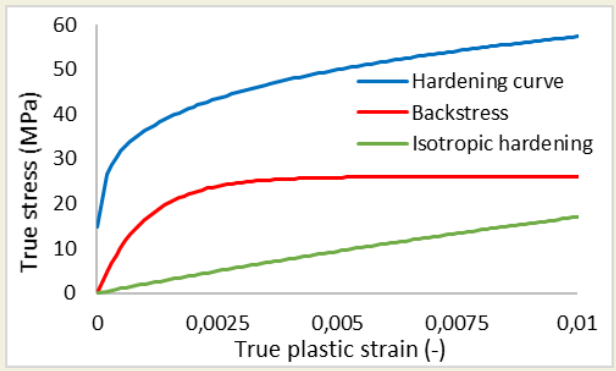

Figure 3. Hardening and backstress curves obtained with curve fitting method

$$\underline{\underline{\alpha}} = \sum_{i=1}^{m}\underline{\underline{\alpha}}^{(i)} \quad (11)$$

In the Eq. (10), dp represents the equivalent plastic strain increment. The parameters h and ζ are similar to the C and γ in the model employed in this work (See in Eq. (7)). h is a material function and expressed as in the Eq. (12).

$$h^{(i)}(p) = h_0^{(i)}\rho(p) \quad (12)$$

In Eq.12 ρ is a function of equivalent plastic strain and defined as,

$$\rho(p) = 1.0 + 2.11\,(1.0 - e^{-9.41p}) \quad (13)$$

Besides, $h_0^{(i)}$ is different for each component of backstress. Isotropic hardening of material is also defined by following expression.

$$Y(p) = Y_0\rho(p) \quad (14)$$

In the equation above, Y_0 is a constant material parameter. Detailed identification procedure was explained in the related article [13].

3.4. FE Modeling

FE simulations of plate with a hole were carried out in commercial Marc software associated with Hypela2 user defined material behavior subroutine. Mechanical properties and the combined hardening parameters were separately incorporated into the subroutine. Fully integrated hexahedral elements which are constant dilatational free from volume locking were utilized to discretize the plate [28, 29]. Owing to the orthotropic symmetry, half section of the plate was generated. Firstly, mesh sensitivity study was carried out by assuming only isotropic hardening. Element number in thickness direction and planar density of the elements were considered, separately. First, for the same planar mesh layout, elements in thickness direction

Table 3. Element numbers in thickness direction of each mesh structure

Case	Total element number	Number of layers in thickness	Solution time[s]
Case 1	1548	2	244
Case 2	3096	4	567
Case 3	6192	8	1369

were increased. Table 3 gives the total element numbers and the number of layers in out of plane direction. Mesh layouts were demonstrated in Fig. 4.

The results of the mesh sensitivity study conducted to investigate the influence of the elements through thickness were shown in Fig. 5 for monotonic loading and cyclic loading separately.

It was seen from the Fig. 5 that the case 2 and case 3 were almost identical. Nonetheless, a dramatic difference was observed between the case 2 and case 3 in terms of the solution time. Therefore, four elements in thickness direction were utilized in line with the case 2 for the further studies. Secondly, the effect of the planar mesh density was assessed. Three different mesh layouts with 4 elements in thickness direction were considered. Element numbers of each mesh layout were given in Table 4, while Fig. 6 gives the mesh layouts used in the planar mesh sensitivity study.

The results of planar mesh sensitivity work were depicted in Fig. 7.

According to the Fig. 7, case 2.2 and case 2.3 were satisfactorily close to each other. Having regard to the solution time, case 2.2 was selected for the further studies.

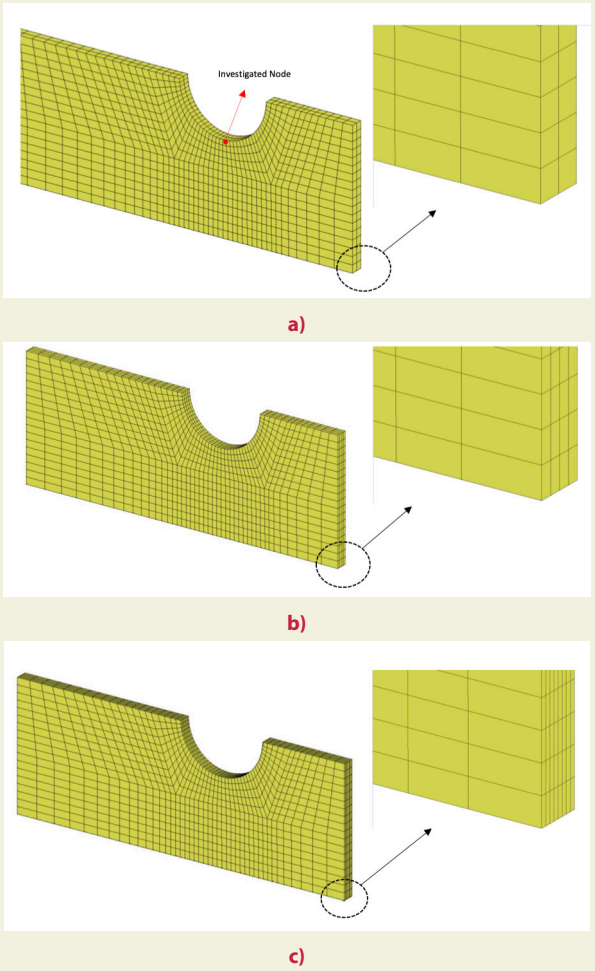

Figure 4. Through thickness elements of the different mesh structures, a) case 1 b) case 2 c) case 3

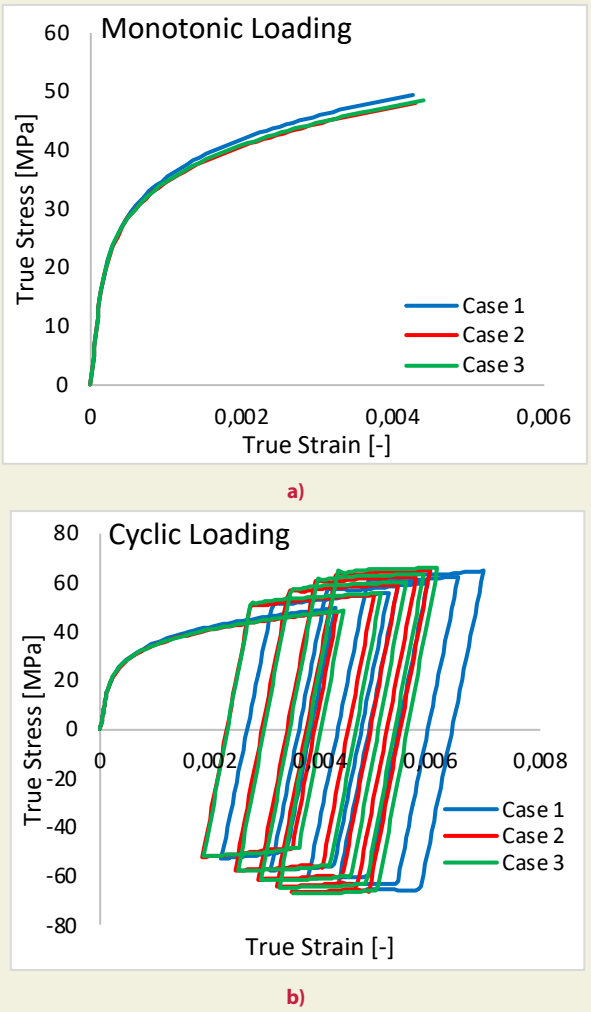

Figure 5. Stress – strain curves obtained from different mesh structures containing different element numbers in out of plane direction a) monotonic loading b) cyclic loading

Table 4. Element numbers of each mesh layout

Case	Total element number	Element number in thickness direction	Solution time[s]
Case 2.1	3096	4	567
Case 2.2	6080	4	1135
Case 2.3	9440	4	1811

4. Results and Discussion

In this section, cyclic deformation of plate with a hole was simulated based on the combined hardening rule assumption. Combined hardening parameters were employed into the Hypela2 user subroutine. The plate was exposed to tension and bending simultaneously. The tensile stress was constant during the process while bending was varying. The results obtained from FE simulation were compared with the Ohno's [13] numerical results. Comparison of the stress – strain curve prediction and the Ohno's result were given in Fig. 8.

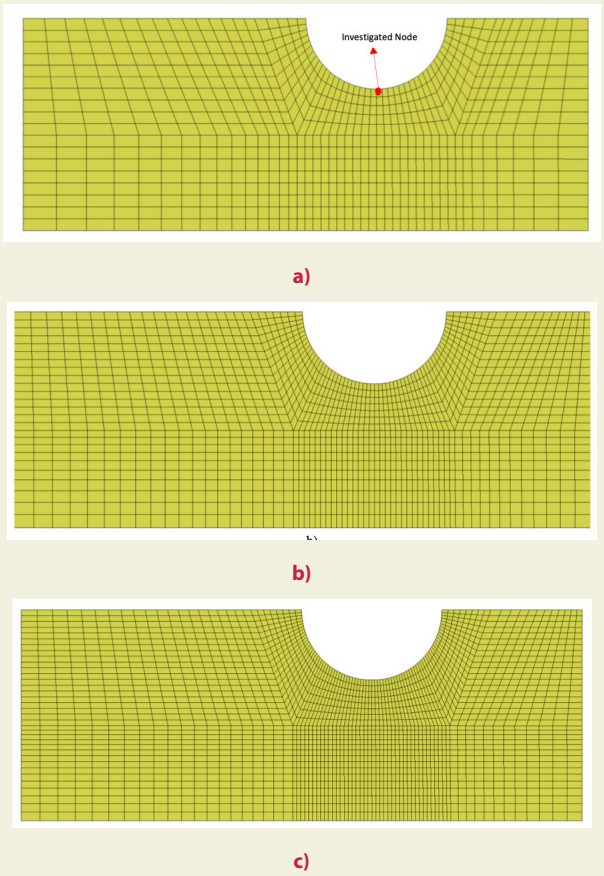

Figure 6. Planar mesh layouts of a) case 2.1 b) case 2.2 c) case 2.3

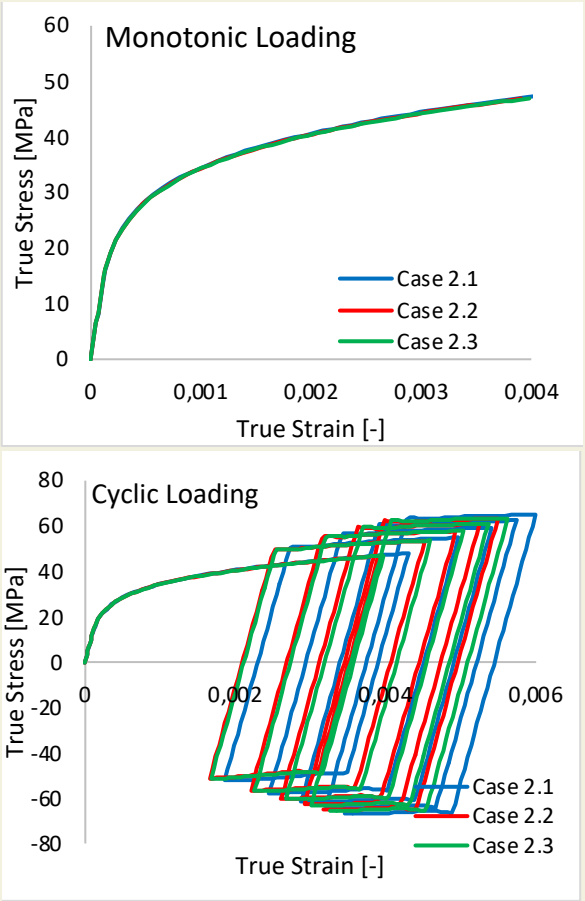

Figure 7. Stress – strain curves obtained from different planar mesh layouts a) monotonic loading b) cyclic loading

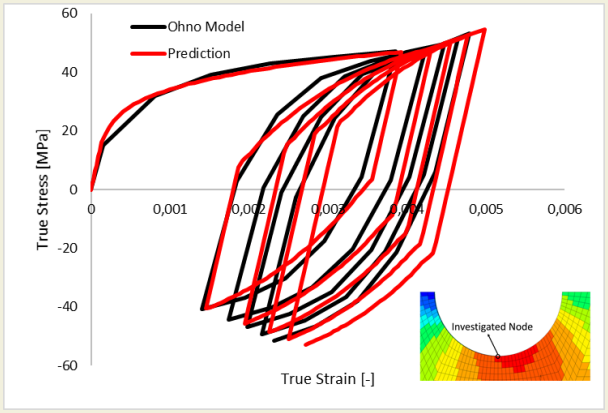

Figure 8. Comparison of the cyclic stress – strain curves obtained from numerical method and Ohno's model

Fig. 8 showed that the Ohno's results were accurately predicted. Especially, stress – strain behavior in the first cycle was entirely captured by the material used in this work. Combined hardening model with AF type kinematic model could address the Bauschinger effect. Moreover, ratcheting behavior of the OFHC copper was tackled by the presence of dynamic recovery – memory term of AF model. Minor discrepancies were observed after the first cycle when compared to the Ohno's result, but these differences were within the small range of error. Loops were inclined to converge in the higher cycles.

5. Conclusions

In the present work, a material model involving a combined isotropic – kinematic hardening model was implemented so as to define the cyclic response of a plate with a hole. The plate is exposed to a constant tensile stress as well as a cyclic bending. Simulations were carried out in commercial Marc software in conjunction with a user subroutine known as Hypela2. The numerical results obtained from the material model used in this work were compared with the Ohno's model [13]. The conclusions were summarized below.

- Bauschinger effect and the ratcheting behavior of the OFHC copper were successfully modeled by the combined hardening model.
- Numerical results obtained from the FE method were in accordance with the Ohno's numeric model. In particular, the first cycle of the cyclic stress – strain curve was accurately captured. The material model used in this work may lead to compatible predictions for the low cycle fatigue applications.
- The loops in cyclic stress strain curve were in tendency to converge which points out that the AF type kinematic hardening model provide a stabilization in loops.
- In the model proposed by Ohno [13], the backstress definition requires a complex calibration procedure and this complex calibration procedure brings about

larger solution times in FE analyses. However, the model employed in this study is more practical and user-friendly. Moreover, presented model provided compatible results in small cyclic strain range when the ratcheting effect is not large.

6. References

[1] Prager, W. (1956). A new method of analyzing stresses and strains in work hardening plastic solids. ASME Journal of Applied Mechanics, 23: 493-496. DOI:10.1115/1.4011389.

[2] Besseling, J.F. (1958). A theory of plastic and creep deformations of an initially isotropic material. ASME Journal of Applied Mechanics, 25: 529-536, DOI:10.1115/1.4011867.

[3] Mroz, Z. (1967). On the description of anisotropic work hardening. Journal of Mechanics and Physics of Solids, 15: 163-175, DOI:10.1016/0022-5096(67)90030-0.

[4] Dafalias, Y.F., Popov, E.F. (1976). Plastic internal variables formalism of cyclic plasticity. ASME Journal of Applied Mechanics, 98: 645-651. DOI:10.1115/1.3423948.

[5] Ohno, N., Wang, J.D., (1993). Kinematic hardening rules with critical state of dynamic recovery. Part 1: Formulations and basic features for ratcheting behavior. International Journal of Plasticity, 9: 375-390. DOI:10.1016/0749-6419(93)90042-O.

[6] Armstrong, P.J., Frederic, C.O. (1966). A mathematical representation of the multiaxial Bauschinger effect. G.E.G.B. Report RD/B/N 731.

[7] Ziegler, H.A. (1959). A modification of Prager's hardening rule. Quarterly of Applied Mechanics, 17: 55-65. DOI:10.1090/qam/104405.

[8] Firat, M. (2011). Notch strain calculation of a notched specimen under axial-torsion loadings. Materials and Design, 32: 3876–3882. DOI:10.1016/j.matdes.2011.03.005.

[9] Firat, M. (2012). Cyclic plasticity modeling and finite element analyzes of a circumferentially notched round bar under combined axial and torsion loadings. Materials and Design, 34: 842-852. DOI:10.1016/j.matdes.2011.07.022.

[10] Aksen, T.A., Esener, E., Firat, M. (2019). Investigation of Notch Root Strain Behaviors Under Combined Loadings, European Journal of Engineering and Natural Sciences, 3: 42-51.

[11] Joo, G., Huh, H. (2018). Rate-dependent isotropic-kinematic hardening model in tension -compression of TRIP and TWIP steel sheets. International Journal of Mechanical Sciences, 146–147: 432–444. DOI:10.1016/j.ijmecsci.2017.08.055.

[12] Joo, G., Huh, H., Choi, M.K. (2016). Tension/compression hardening behaviors of auto-body steel sheets at intermediate strain rates. International Journal of Mechanical Sciences, 108-109: 174–187. DOI:10.1016/j.ijmecsci.2016.01.035.

[13] Ohno, N., Tsuda, M., Kamei, T. (2013). Elastoplastic implicit integration algorithm applicable to both plane stress and three-dimensional stress states. Finite Elements in Analysis and Design, 66:1–11. DOI: 10.1016/j.finel.2012.11.001.

[14] Zhang, M., Benitez, J.M., Montáns, F.J. (2018). Cyclic plasticity using Prager's translation rule and both nonlinear kinematic and isotropic hardening: Theory, validation, and algorithmic implementation. Computer Methods in Applied Mechanics and Engineering, 328:565–593. DOI:10.1016/j.cma.2017.09.028.

[15] Zhang, M., Montáns, F.J., (2019). A simple formulation for large-strain cyclic hyperelasto-plasticity using elastic correctors. Theory and algorithmic implementation. International Journal of Plasticity, 113: 185–217. DOI:10.1016/j.ijplas.2018.09.013.

[16] Fu, S., Yu, D., Chen, G., Chen, X. (2016). Ratcheting of 316L stainless steel thin wire under tension-torsion loading. Fracture and Structural Integrity, 38: 141-147. DOI:10.3221/IGF-ESIS.38.19.

[17] Shojaei, A., Eslami, M.R., Mahbadi, H. (2010). Cyclic loading of beams based on the Chaboche model. International Journal of Mechanics and Materials in Design, 6:217–228. DOI:10.1007/s10999-010-9131-5.

[18] Badnava, H., Pezeshki, S.M., Nejad, F., Farhoudi, H.R. (2012). Determination of combined hardening material parameters under strain controlled cyclic loading by using the genetic algorithm method. Journal of Mechanical Science and Technology, 26(10):3067~3072. DOI:10.1007/s12206-012-0837-1.

[19] Tasavori, M., Zehsaz, M., Tahami, F.V. (2020). Ratcheting assessment in the tube sheets of heat exchangers using the nonlinear isotropic/kinematic hardening model. International Journal of Pressure Vessels and Piping, 183:104-103. DOI:10.1016/j.ijpvp.2020.104103.

[20] Nath, A., Ray, K.K., Barai, V. (2019). Evaluation of ratcheting behaviour in cyclically stable steels through use of a combined kinematic-isotropic hardening rule and a genetic algorithm optimization technique. International Journal of Mechanical Sciences, 152:138–150. DOI:10.1016/j.ijmecsci.2018.12.047.

[21] Lee, E., Stoughton, T.B., Yoon, J.W. (2019). Kinematic hardening model considering directional hardening response. International Journal of Plasticity, 110:145–165. DOI:10.1016/j.ijplas.2018.06.013.

[22] Qin, J., Holmedal, B., Hopperstad, O.S. (2018). A combined isotropic, kinematic, and distortional hardening model for aluminum and steels under complex strain-path changes. International Journal of Plasticity, 101: 156–169. DOI:10.1016/j.ijplas.2017.10.013.

[23] Shahabi, M., Nayebi, A. (2015). Springback modeling in L-Bending process using continuum damage mechanic's concept. Journal of Applied and Computational Mechanics, 1: 161-167. doi: 10.22055/jacm.2015.11020.

[24] Meggiolaro, M.A., Castro, J.T.P., Wu, H. (2015). On the applicability of multi-surface, two-surface and non-linear kinematic hardening models in multiaxial fatigue. Fracture and Structural Integrity, 33: 357-367. DOI: 10.3221/IGF-ESIS.33.39.

[25] Chen, J., Xiao, Y., Ding, W., Zhu, X. (2015). Describing the non-saturating cyclic hardening behavior with a newly developed kinematic hardening model and its application in springback prediction of DP sheet metals. Journal of Materials Processing Technology, 215: 151–158. DOI:10.1016/j.jmatprotec.2014.08.014.

[26] Adin, H., Sağlam, Z,. & Adin, M.Ş. (2021). Numerical Investigation of Fatigue Behavior of Non-patched and Patched Aluminum/Composite Plates. European Mechanical Sci-

ence, 5 (4): 168-176 . DOI: 10.26701/ems.923798.

[27] Paul, S.K., Sivaprasad, S., Dhar, S., Tarafder, M., Tarafder, S. (2010). Simulation of cyclic plastic deformation response in SA333 C-Mn steel by a kinematic hardening model. Computational Materials Science, 48: 662-671. DOI:10.1016/j.commatsci.2010.02.037.

[28] Marc 2018.1 Volume A: Theory and User Manual.

[29] Marc 2018.1 Volume B: Element Library.